

Soliton mode-locked Nd:YAlO₃ laser at 930 nm

T. Kellner, F. Heine,* and G. Huber

Institut für Laser-Physik, Universität Hamburg, Jungiusstrasse 9a, D-20355 Hamburg, Germany

C. Hönninger, B. Braun, F. Morier-Genoud, M. Moser, and U. Keller

Ultrafast Laser Physics, Institute of Quantum Electronics, ETH-Hönggerberg HPT, CH-8093 Zürich, Switzerland

Received November 20, 1997

We report on a soliton mode-locked Nd:YAlO₃ laser at 930 nm. We used a semiconductor saturable absorber mirror and a Gires–Tournois Interferometer for dispersion compensation to achieve soliton mode locking. The generated pulses were as short as $\Delta\tau_{\text{FWHM}} = 1.9$ ps with a spectral bandwidth of $\Delta\lambda = 0.5$ nm. The pulses were almost transform limited assuming a sech^2 pulse shape. The averaged output power was 410 mW at an absorbed pump power level of 1.76 W. An investigation of the effect of the third-order dispersion of the Gires–Tournois interferometer on the spectra of the mode-locked laser is presented. © 1998 Optical Society of America [S0740-3224(98)02205-X]

OCIS codes: 140.3580, 140.4050, 140.7090.

1. INTRODUCTION

Many efforts have been made in recent years to develop an all-solid-state blue laser source. Semiconductor diode-pumped solid-state lasers in combination with nonlinear techniques, such as frequency doubling or sum-frequency mixing, are well-investigated approaches to obtain a coherent light source in the blue spectral region. Frequency doubling of the ground-state laser transition (${}^4F_{3/2} \rightarrow {}^4I_{9/2}$) in neodymium-doped YAG has yielded the highest continuous-wave (cw) output power at 473 nm so far.^{1,2} An alternative to cw operation is mode locking of this transition in order to take advantage of the high fundamental peak power and to increase the frequency-doubling efficiency. Hofer *et al.*³ have recently demonstrated mode-locked operation in a Nd-doped fiber laser at 920 nm with a laser output power of 85 mW.

The ground-state laser transition in neodymium-doped laser hosts has some inherent difficulties owing to the quasi-three-level nature of this laser system. Only a host material with a large ground-state splitting and a good thermal conductivity allows efficient laser operation. Furthermore, a short gain length and a high pump brightness are necessary. These requirements are met in an end-pumped configuration.

Nd:YAlO₃ is a promising material to achieve short-pulse operation on the ${}^4F_{3/2} \rightarrow {}^4I_{9/2}$ transition because of the spectral bandwidth and the lifetime of the upper laser level. The spectral bandwidth of the fluorescence peak at 930 nm of $\Delta\lambda_{\text{FWHM}} = 2.5$ nm is broader than the fluorescence bandwidth of the ground-state transition of the commonly used Nd:YAG ($\Delta\lambda_{\text{FWHM}} = 1$ nm at 946 nm). In addition, the lifetime of the upper laser level $\tau = 160$ μs is shorter when compared with other neodymium-doped laser hosts like Nd:YLiF₄ or Nd:YAG. This lowers the tendency of Q-switched mode locking in passively mode-locked lasers.⁴ The Nd:YAlO₃ crystal has an orthorhombic lattice with space group D_{2h}^{16} . The as-

ignment of the crystallographic axes follows the $Pnma$ notation. The lattice constants are given by $a = 5.139$ Å, $b = 7.370$ Å, and $c = 5.179$ Å. The thermal conductivity is approximately the same as in Nd:YAG. However, the ground-state splitting is smaller than in Nd:YAG, which results in an increased reabsorption loss and therefore in a higher laser threshold.

In this paper we report soliton mode-locked operation in Nd:YAlO₃ at 930 nm. Soliton mode locking was achieved by using a semiconductor saturable absorber mirror⁵ (SESAM) and a Gires–Tournois interferometer⁶ (GTI). The SESAM started the pulse-formation process and stabilized the soliton. The soliton pulse is formed by the interplay between the self-phase modulation (SPM) in the cavity and the negative group-velocity dispersion (GVD) introduced by the GTI.

2. EXPERIMENT

Figure 1 shows a schematic of the laser setup for the mode-locking experiments. The 2-mm-long flat Brewster-cut Nd(0.8%):YAlO₃ crystal was cut for laser operation polarized parallel to the crystallographic a axis ($\mathbf{k}||c$ axis). This plane of polarization exhibits the highest emission cross section of $\sigma_{\text{em}} = 4.1 \times 10^{-20}$ cm^2 . The flat facet of the crystal was coated for high reflection at 930 nm and for high transmission at the pump wavelength. The coating has also a transmission higher than 90% between 1.05 μm and 1.1 μm to avoid laser oscillation at 1.08 μm on the ${}^4F_{3/2} \rightarrow {}^4I_{11/2}$ transition in Nd:YAlO₃. A Ti:sapphire laser operating at 813 nm was used as a pump source. The absorption coefficient parallel to the crystallographic a axis of Nd(0.8%):YAlO₃ at 813 nm is $\alpha = 10$ cm^{-1} . We mounted the crystal on a TE cooler to achieve an efficient heat removal.

The SESAM⁵ consists of an absorbing layer of InGaAs with a thickness of 15 nm placed between two transparent layers of GaAs. These layers were grown on a high-

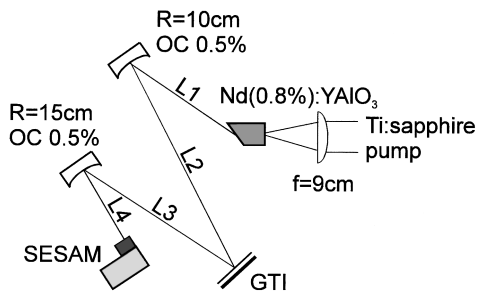


Fig. 1. Nd:YAlO₃ laser setup with a GTI and a SESAM. $L_1 = 5.7$ cm, $L_2 = 30$ cm, $L_3 = 39$ cm, and $L_4 = 9.2$ cm. OC, output coupler.

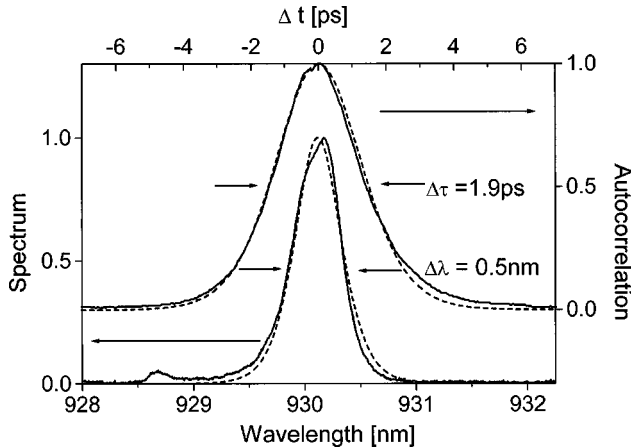


Fig. 2. Pulse width and spectrum of the mode-locked Nd:YAlO₃ laser at 930 nm at an incident pump power level of 2.38 W. The dashed curves are fits to an ideal sech² pulse shape.

reflecting Bragg mirror consisting of 25 pairs of quarter-wave layers of GaAs and AlAs. The thickness of the transparent layers was chosen to ensure that the absorbing layer is located at an antinode of the standing wave inside the SESAM. The saturable absorber exhibits a bi-temporal impulse response with a fast component of approximately $\tau_f = 200$ fs and a slow component of $\tau_s = 12$ ps. The GTI is a Fabry–Perot structure consisting of a high-reflecting end mirror and a mirror with 4% reflection separated by a distance of approximately 80 μm . The mirror spacing was varied by piezoelectric transducers. The spot radius on the SESAM ($\omega = 48$ μm) and the elliptical laser mode inside the Nd:YAlO₃ crystal ($\omega_x = 63$ μm , $\omega_y = 34$ μm) were calculated by use of an ABCD matrix formalism.

For cw laser experiments we replaced the GTI by a flat output coupler ($T_{oc} = 1\%$), which led to a total output coupling of 2%. The curved mirrors in the cw laser experiment were coated to be high reflecting at $\lambda = 930$ nm. A maximum laser output power of 570 mW was achieved in the cw mode at an absorbed pump power level of 1.55 W. The slope efficiency was 47%. The spectral bandwidth of the laser in the cw mode was $\Delta\lambda_{cw} = 0.45$ nm.

In the mode-locking experiments, pulses as short as $\Delta\tau_{FWHM} = 1.9$ ps at 930 nm (see Fig. 2) were generated. The pulse repetition rate was 178 MHz. The total average output power was 410 mW at an absorbed pump

power level of 1.76 W. The spectral bandwidth was 0.5 nm (Fig. 2) corresponding to a time–bandwidth product of 0.33, which is nearly transform limited assuming a sech² pulse. Usually, the pulses in end-pumped mode-locked laser systems are not transform limited. The reason for this is the enhanced spatial hole burning in comparison to laser systems with the gain medium in the center of a standing-wave cavity.⁷ However, it was predicted that soliton mode locking with nearly-transform-limited pulses in end-pumped laser systems is possible if the SPM is increased, while negative group-velocity dispersion is introduced in the cavity.⁸

Figure 3 shows the spectral characteristics of the mode-locked laser for different spectral voltages of the GTI (i.e., different mirror spacings) at the same incident pump power of $P_{in} = 1.86$ W. By varying the mirror spacing, it is possible to adjust the total amount of negative GVD necessary to compensate for (i) the SPM in the laser crystal, (ii) the positive GVD of the mirror coatings, and (iii) the positive GVD owing to the material dispersion in the laser crystal. The positive GVD of the mirrors at 930 nm was measured to be only $D_{mirror} \approx 200$ fs² per roundtrip. The dispersion measurement was made with a white-light interferometer. The laser crystal's GVD was calculated to be 95 fs² per single pass with the refractive index data for Nd:YAlO₃ from Kuwano.⁹ The autocorrelation traces of the pulses to the corresponding spectra are depicted in the insets of Fig. 3. No pulse-form distortion was observed for a decreased negative GVD of the GTI. The linear behavior of the pulse width versus the GTI voltage (see Fig. 4) indicates that the GTI operates in the linear-dispersion regime. From the soliton equation¹⁰

$$\Phi = \frac{D_2}{2\tau^2}, \quad (1)$$

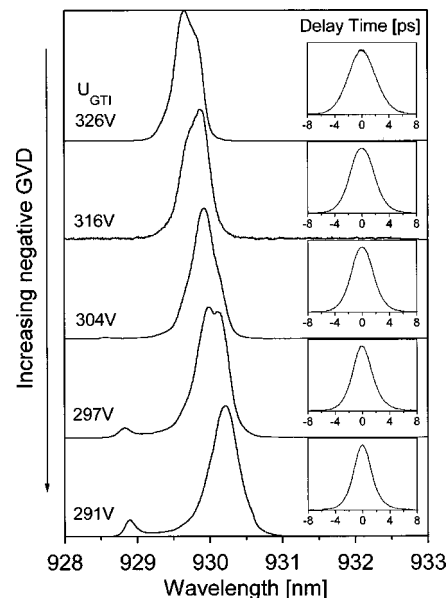


Fig. 3. Mode-locked spectra of the Nd:YAlO₃ laser for different voltages of the GTI, i.e., different amounts of negative GVD. The autocorrelation traces of the corresponding spectra are depicted in the insets.

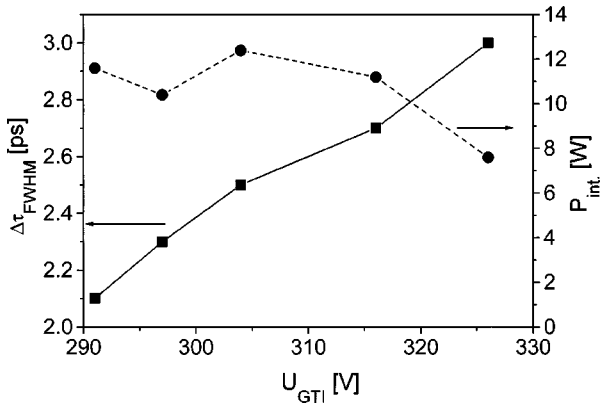


Fig. 4. Pulse width and calculated intracavity power versus voltage of the GTI at an incident pump power level of 1.86 W.

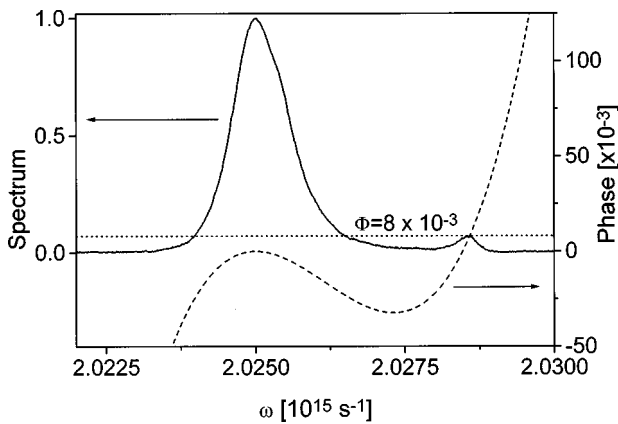


Fig. 5. Spectra of the pulse of Fig. 2 in the frequency domain (solid curve). Phase of the GTI (dashed curve) including GVD and third-order dispersion and the nonlinear phase shift (dotted line) owing to the Kerr effect in the Nd:YAlO₃ crystal.

we obtained an expression for the dependence of the pulse width τ on the intracavity GVD given by D_2 . The pulse duration is given by $\tau = \tau_{\text{FWHM}}/1.76$. The phase shift Φ of the soliton per round trip can be calculated by $\Phi = \frac{1}{2} \delta |A_0|^2 = \frac{1}{4} \delta (E_p/\tau)$. E_p is the pulse energy, and δ is the SPM coefficient. This yields a linear relationship between the pulse width and the intracavity GVD D_2 , i.e.,

$$\tau = \frac{4D_2}{2\delta E_p}. \quad (2)$$

The intracavity power decreases at a pulse width of $\Delta\tau_{\text{FWHM}} = 3$ ps (Fig. 4). The laser stopped mode locking if the GTI voltage was further increased. Without dispersion compensation, no stable mode locking was observed. The SPM and the uncompensated positive GVD of the mirrors and the laser crystal leads to pulse distortion in the absence of a negative GVD. With the help of Eq. (1) we calculate the intracavity GVD D_2 . The SPM coefficient δ is given by the expression

$$\delta = \frac{2\pi}{\lambda} \gamma \frac{2L_g}{A_{\text{eff}}}. \quad (3)$$

λ is the laser wavelength (in free space), γ is the Kerr-index nonlinearity, L_g is the length of the gain medium, and A_{eff} is the mode area in the laser crystal. The Kerr-index nonlinearity of YAlO₃ is $\gamma = 7.3 \times 10^{-16} \text{ cm}^2/\text{W}$.¹¹ We obtained $D_2 \approx 19.000 \text{ fs}^2$ for an intracavity pulse energy of 119 nJ (Fig. 2). The negative GVD of the GTI with a mirror spacing between 79.71 μm and 79.75 μm is in the range of 5000 fs^2 to 20.000 fs^2 . This yields a negative GVD of 10.000 fs^2 to 40.000 fs^2 because of two reflection at the GTI per roundtrip. This is in good agreement with the calculated value for D_2 from Eq. (1). However, this result shows that the GTI's mirror spacing is critical to adjust to obtain the necessary amount of negative GVD for stable mode locking. In experiments with an increased effective mode area in the laser crystal (which reduces the nonlinear phase shift owing to the SPM) we obtained no stable mode locking without dispersion compensation.

The sidebands in the mode-locked spectra at 930 nm (Fig. 2 and Fig. 3) that appear for shorter pulses (i.e., reduced voltages) can be explained by the third-order dispersion of the GTI. This spectral behavior was previously observed in femtosecond Ti:sapphire lasers,¹² in mode-locked dye lasers,¹³ and in femtosecond Cr:LiSAF lasers.^{14,15} A theoretical analysis was given by Haus *et al.*¹⁶ for passively mode-locked lasers. The sideband corresponds to a dispersive wave that extracts energy from the short pulse. This process is only efficient if the two waves are phase matched. The phase-matching condition is given by

$$\Phi = (\omega - \omega_0)^2 \frac{D_2}{2} + (\omega - \omega_0)^3 \frac{D_3}{6}, \quad (4)$$

D_3 is the third-order-dispersion coefficient of the GTI, and ω_0 is the center frequency of the soliton. For the calculation of the phase-matching condition (4) we considered the positive GVD of the mirrors and the laser crystal, but we neglected the dispersion of the SESAM. The results of the calculation are shown in Fig. 5 for a GTI mirror spacing of 79.718 μm . The intersection of the nonlinear phase shift and the dispersion curve of the GTI is in good agreement with the spectral sideband of the mode-locked laser.

3. CONCLUSIONS

In summary, we have demonstrated a Ti:sapphire-pumped soliton mode-locked Nd:YAlO₃ laser at 930 nm. Mode locking was achieved by use of a semiconductor saturable absorber mirror and a Gires-Tournois interferometer for dispersion compensation. We observed pulses as short as $\Delta\tau_{\text{FWHM}} = 1.9$ ps with a spectral bandwidth of $\Delta\lambda = 0.5$ nm. The pulses were almost transform limited assuming a sech^2 pulse shape. The total output power was 410 mW at an input pump power of 2.38 W. It was shown that the generation of a dispersive wave, which results in a spectral sideband in the mode-locked laser spectra, was a result of the third-order dispersion of the GTI.

Future work will be concentrated on laser diode pumping, investigations of different laser hosts like Nd:YLiF₄,

and extracavity frequency doubling of the mode-locked laser into the blue spectral region.

ACKNOWLEDGMENT

This work was supported by the German Ministry for Education and Research (Bundesministerium für Bildung und Forschung project 16SV094/3) and the Swiss priority program in optics. The authors thank D. Sutter for the dispersion measurements of the mirrors.

*Present address: Bosch Telecom GmbH, Gerberstrasse 33, 71549 Backnang, Germany.

REFERENCES

1. T. Kellner, F. Heine, and G. Huber, "Efficient laser performance of Nd:YAG at 946nm and intracavity frequency doubling with LiJO_3 , $\beta\text{-BaB}_2\text{O}_4$, and LiB_3O_5 ," *Appl. Phys. B* **65**, 789–792 (1997).
2. M. Bode, I. Freitag, A. Tünnermann, and H. Welling, "Frequency-tunable 500-mW continuous-wave all-solid-state single-frequency source in the blue spectral region," *Opt. Lett.* **19**, 1220–1222 (1997).
3. R. Hofer, M. Hofer, G. A. Reider, M. Cernusca, and M. H. Ober, "Modelocking of a Nd-fiber laser at 920 nm," *Opt. Commun.* **140**, 242–244 (1997).
4. F. X. Kärtner, L. R. Brovelli, D. Kopf, M. Kamp, I. Calasso, and U. Keller, "Control of solid state laser dynamics by semiconductor devices," *Opt. Eng. (Bellingham)* **34**, 2024–2036 (1995).
5. U. Keller, K. J. Weingarten, F. X. Kärtner, D. Kopf, B. Braun, I. D. Jung, R. Fluck, C. Hönninger, N. Matuschek, and J. Aus der Au, "Semiconductor saturable absorber mirrors (SESAM's) for femtosecond to nanosecond pulse generation in solid-state-lasers," *IEEE J. Sel. Top. Quantum Electron.* **2**, 435–453 (1996).
6. F. Gires and P. Tournois, "Interféromètre utilisable pour la compression d'impulsion lumineuses modulées en fréquence," *C. R. Acad. Sci.* **258**, 6112–6115 (1964).
7. B. Braun, K. J. Weingarten, F. X. Kärtner, and U. Keller, "Continuous-wave mode-locked solid-state lasers with enhanced spatial hole burning. I. Experiment," *Appl. Phys. B* **61**, 429–437 (1995).
8. F. X. Kärtner, B. Braun, and U. Keller, "Continuous-wave mode-locked solid-state lasers with enhanced spatial hole burning. II. Theory," *Appl. Phys. B* **61**, 569–579 (1995).
9. Y. Kuwano, "Refractive indices of $\text{YAlO}_3\text{:Nd}$," *J. Appl. Phys.* **49**, 4223–4224 (1978).
10. F. X. Kärtner and U. Keller, "Stabilization of solitonlike pulses with a slow saturable absorber," *Opt. Lett.* **20**, 16–18 (1995).
11. R. Adair, L. L. Chase, and S. A. Payne, "Nonlinear refractive index of optical crystals," *Phys. Rev. B* **39**, 3337–3350 (1989).
12. P. F. Curley, Ch. Spielmann, T. Brabec, F. Krausz, E. Wintner, and A. J. Schmidt, "Operation of a femtosecond Ti:sapphire solitary laser in the vicinity of zero group-delay dispersion," *Opt. Lett.* **18**, 54–56 (1993).
13. F. W. Wise, I. A. Walmsley, and C. L. Tang, "Simultaneous formation of solitons and dispersive waves in a femtosecond ring dye laser," *Opt. Lett.* **13**, 129–131 (1988).
14. M. J. P. Dymott and A. J. Ferguson, "Pulse duration limitations in a diode-pumped femtosecond Kerr-lens mode-locked Cr:LiSAF laser," *Appl. Phys. B* **65**, 227–234 (1997).
15. I. T. Sorokina, E. Sorokin, E. Wintner, A. Cassanho, H. P. Jenssen, and R. Szipöcs, "Sub-20 fs pulse generation from the mirror dispersion controlled Cr:LiSGaF and Cr:LiSAF lasers," *Appl. Phys. B* **65**, 245–253 (1997).
16. H. A. Haus, J. D. Moores, and L. E. Nelson, "Effect of the third-order dispersion on passive mode locking," *Opt. Lett.* **18**, 51–53 (1993).